



HAL
open science

A positive and asymptotic preserving finite volume scheme for the linear transport equation on two dimensional unstructured meshes

Clément Lasuen

► **To cite this version:**

Clément Lasuen. A positive and asymptotic preserving finite volume scheme for the linear transport equation on two dimensional unstructured meshes. 2024. hal-04336178v2

HAL Id: hal-04336178

<https://hal.science/hal-04336178v2>

Preprint submitted on 13 May 2024

HAL is a multi-disciplinary open access archive for the deposit and dissemination of scientific research documents, whether they are published or not. The documents may come from teaching and research institutions in France or abroad, or from public or private research centers.

L'archive ouverte pluridisciplinaire **HAL**, est destinée au dépôt et à la diffusion de documents scientifiques de niveau recherche, publiés ou non, émanant des établissements d'enseignement et de recherche français ou étrangers, des laboratoires publics ou privés.

A positive and asymptotic preserving finite volume scheme for the linear transport equation on two dimensional unstructured meshes

Clément Lasuen¹

¹CEA, DAM, DIF, F-91297 Arpajon, France

`clement.lasuen@gmail.com`

May 13, 2024

Abstract

In this paper, we propose a finite volume scheme for the linear transport equation in two space dimensions. This scheme is based on an upwind scheme where the velocity is modified so as to recover the correct diffusion limit. The resulting scheme is *asymptotic preserving*, positive under a classical *CFL* condition and conservative. We propose a reconstruction procedure so as to make it second order consistent on unstructured polygonal meshes.

Contents

| | | |
|----------|---------------------------------------------------------|-----------|
| 1 | Introduction | 3 |
| 2 | Notations assumptions on the mesh | 5 |
| 3 | Upwind scheme | 7 |
| 3.1 | Properties | 8 |
| 3.2 | Dirichlet boundary conditions | 9 |
| 3.3 | Periodic boundary conditions | 9 |
| 4 | Numerical scheme | 9 |
| 4.1 | Upwind scheme and modified streaming velocity | 10 |
| 4.2 | Partially implicit time discretisation | 11 |
| 4.3 | Properties | 12 |
| 4.4 | <i>AP</i> property and limit scheme | 13 |
| 5 | Numerical results | 14 |
| 5.1 | Free streaming regime | 14 |
| 5.2 | Diffusion regime | 15 |
| 5.3 | Manufactured test case | 15 |
| 5.4 | Lattice problem | 16 |
| 5.5 | Variable scattering test case | 17 |
| 6 | Conclusion and future work | 18 |
| 7 | Appendix | 18 |
| 7.1 | Proof of Lemma 3.1 | 18 |
| 7.2 | Proof of Lemma 3.2 | 19 |
| 7.3 | Proof of Lemma 4.1 | 20 |

1 Introduction

In this work, we propose a finite volume scheme that discretises the radiative transfer equation (see [MM84]):

$$\frac{1}{c} \partial_t I + \operatorname{div} (I \boldsymbol{\omega}) + \sigma^t I = \sigma^s \frac{1}{4\pi} \int_{\mathcal{S}^2} I d\boldsymbol{\omega}' + q. \quad (1)$$

It is a linear Boltzmann type equation. The unknown $I = I(t, \mathbf{x}, \boldsymbol{\omega})$ is the radiative intensity and gives the distribution of photons. It depends on the time variable $t \geq 0$, on the space variable $\mathbf{x} \in \Omega \subset \mathbb{R}^3$ (Ω being the computational domain) and direction $\boldsymbol{\omega} \in \mathcal{S}$, where \mathcal{S} is the unit sphere in \mathbb{R}^3 . The source term $q = q(t, \mathbf{x}, \boldsymbol{\omega}) \geq 0$ is nonnegative. The scattering cross section is $\sigma^s \geq 0$ and the total cross section is $\sigma^t \geq \sigma^s$. The difference $\sigma^t - \sigma^s = \sigma^a$ is the absorption cross section. We assume here that the speed of light c is equal to 1.

Equation (1) is of great importance in the numerical simulation of inertial confinement fusion (ICF). In these experiments, a small ball of hydrogen (the target) is submitted to intense radiation by laser beams. These laser beams are either pointed directly to the target (direct drive approach), or pointed to gold walls of a hohlraum in which the target is located (indirect drive approach, see Figure 1). These gold walls heat up, emitting X-rays toward the target. The outer layers of the target are heated up, hence ablated. By momentum conservation, the inner part of the target implodes (this is usually called the rocket effect). Hence, the pressure and temperature of the hydrogen inside the target increase, hopefully reaching the thermodynamical conditions for nuclear fusion. This process is summarized in Figure 2. Other possible applications of (1) are radiation hydrodynamics in stellar atmospheres. Of course, the model (1) is over-simplified for these applications as it should, among other things, include a dependence on the frequency. But (1) should be seen as an elementary building block for more realistic models.

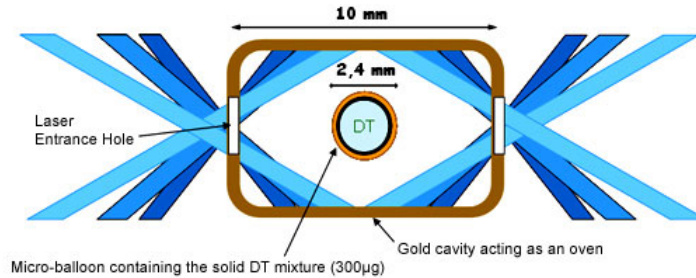


Figure 1: Schematic view of the Hohlraum and the target

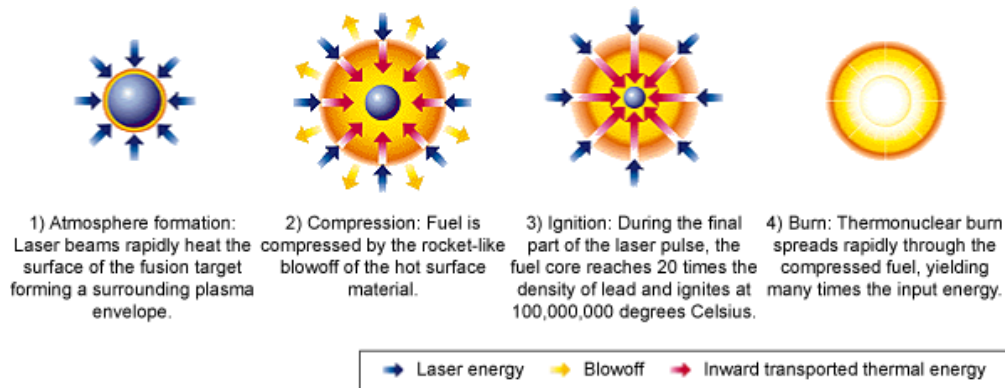


Figure 2: The concept of ICF (inertial confinement fusion) taken from <http://www.lanl.gov/projects/dense-plasma-theory/background/dense-laboratory-plasmas.php>

It has been shown in [CZ67] that if $q > 0$ and $\sigma^t > 0$ and $\sigma^a > 0$ then the solution I is positive. Moreover, in [RJLM⁺88] the author proved that if $q = 0$ and $\sigma^t = \sigma^s$ then the solution satisfies a maximum principle property.

Eventually, Equation (1) admits a diffusion limit. Let $\varepsilon > 0$ be given. If we replace $\sigma^s \leftarrow \sigma^s/\varepsilon$, $\sigma^a \leftarrow \sigma^a\varepsilon$, $q \leftarrow q\varepsilon$ and if we perform the following scaling $t \leftarrow \varepsilon t$, then (1) reads as:

$$\partial_t I + \frac{1}{\varepsilon} \operatorname{div} (I\omega) + \frac{\sigma^t}{\varepsilon^2} I = \frac{\sigma^s}{\varepsilon^2} \frac{1}{4\pi} \int_{S^2} I d\omega' + q, \quad (2)$$

with $\sigma^t = \sigma^s + \varepsilon^2 \sigma^a$. Moreover, when ε vanishes, the solution I of (2) converges toward the solution of a diffusion equation $I \xrightarrow{\varepsilon \rightarrow 0} E^0$ where:

$$\partial_t E^0 - \operatorname{div} \left(\frac{1}{3\sigma^s} \nabla E^0 \right) + \sigma^a E^0 = \frac{1}{4\pi} \int_{S^2} q d\omega'. \quad (3)$$

See [BGPS88] [Cas04]. Therefore it is important for a numerical scheme that discretises (2) to be consistent with the limit model (3). In this case, we say that the scheme is *asymptotic-preserving*. More precisely, the parameter $\varepsilon \in [0, 1]$ characterizes the proportion between the streaming and diffusion phenomena. The configuration $\varepsilon = 1$ corresponds to the free streaming regime and $\varepsilon = 0$ to the pure diffusion regime. We use the notations of Figure 3 and we denote by h the discretisation parameter. The general model (2) is denoted by P^ε and it is discretised with the scheme P_h^ε . The model P^ε tends towards the diffusion limit model P^0 (Equation (3)) when $\varepsilon \rightarrow 0$. We want the limit scheme P_h^0 (obtained by setting $\varepsilon \rightarrow 0$ in P_h^ε) to be consistent with P^0 . If this property is fulfilled, then we say that the scheme P_h^ε is *asymptotic preserving* or *AP*. We emphasize that ε is present in the equations through ε^{-1} , hence the corresponding terms are stiff in the diffusion limit ($\varepsilon \rightarrow 0$). The diffusion limit is thus a singular limit. This explains both why the limit equation is of different nature and why designing AP schemes is not trivial.

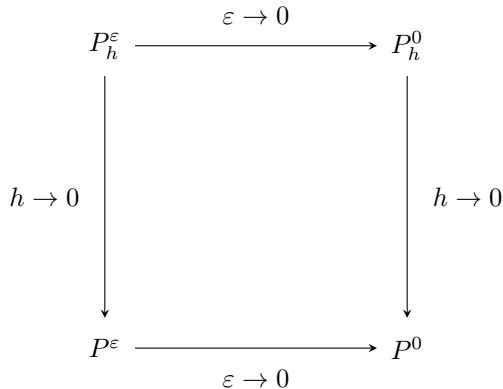


Figure 3: Definition of an *AP* scheme.

The very first works in this direction were [LM89] and [JL96]. These papers were dedicated to *1D* calculations. One dimensional finite difference methods that solved (2) were proposed in [Kla98, JPT00] for instance. The work [KFJ16] proposes an extension of these methods to the two dimensional case. The space and angular variable are both discretised on uniform grids and a time splitting discretisation method (IMEX method, see for instance [BFR16, BR09, EG23]) is performed.

The discontinuous finite elements method was also used to solve (2) on two and three dimensional unstructured meshes. See [Ada01] [BCWA] [CS16] for instance. These methods are consistent but not positive. A recent work [GPR20] proposes a positive, *AP* and first order scheme to solve the stationary version of (2). Micro-macro decompositions were also used to solve (2) on uniform grids. See for instance [LFH19, LM08, LM10, JS10, EHW21]. Recently, [ACE⁺22] proposed an *AP* finite volume scheme that is based on a micro-macro decomposition. The scheme is first order consistent on *2D* unstructured meshes but it is not positive.

In this paper we propose a method that:

- is asymptotic preserving: the scheme we obtain when $\varepsilon \rightarrow 0$ is consistent with (3),
- is second order consistent on unstructured $2D$ meshes for any ε ,
- preserves the positivity of the numerical solution under a classical *CFL* condition,
- has a compact stencil,
- is conservative,
- has the same computational cost as an explicit scheme: there is no linear system to invert nor fixed-point iteration to compute.

We perform an angular discretisation of (2). We choose K directions $(\boldsymbol{\omega}_k)_{1 \leq k \leq K}$ and we define $I_k = I(t, \mathbf{x}, \boldsymbol{\omega}_k)$ for $1 \leq k \leq K$. The integral over the unit sphere in (2) is discretised as:

$$\frac{1}{4\pi} \int_{S^2} Id\boldsymbol{\omega}' \approx \sum_{k'=1}^K p_{k'} I_{k'}.$$

The quadrature weights $(p_k)_{1 \leq k \leq K}$ and the directions $(\boldsymbol{\omega}_k)_{1 \leq k \leq K}$ are required to satisfy:

$$p_k \geq 0, \quad \sum_{k'=1}^K p_{k'} = 1, \quad \sum_{k'=1}^K p_{k'} \boldsymbol{\omega}_{k'} = \mathbf{0}, \quad \sum_{k'=1}^K p_{k'} \boldsymbol{\omega}_{k'} \otimes \boldsymbol{\omega}_{k'} = \frac{1}{3} \begin{pmatrix} 1 & 0 & 0 \\ 0 & 1 & 0 \\ 0 & 0 & 1 \end{pmatrix}. \quad (4)$$

The equation we solve therefore reads as:

$$\partial_t I_k + \frac{1}{\varepsilon} \operatorname{div} (I_k \boldsymbol{\omega}_k) + \frac{\sigma^t}{\varepsilon^2} I_k = \frac{\sigma^s}{\varepsilon^2} \sum_{k'=1}^K p_{k'} I_{k'} + q_k. \quad (5)$$

Moreover, owing to (4), when ε vanishes, Equation (5) admits a diffusion limit: $I_k \xrightarrow[\varepsilon \rightarrow 0]{} E^0$ where E^0 is solution to (3).

In this work, we focus on the two dimensional case. We briefly explain in the conclusion that our methodology can be easily extended to the three dimensional case.

The main idea of our method is to use an upwind scheme to discretise Equation (5) and to modify the streaming velocity in order to obtain a scheme that is consistent with (3) when $\varepsilon \rightarrow 0$. The scheme is said to be *composite* as the fluxes are computed at the nodes and at the edges of the cells (this idea was first introduced in [BCHS20, Hoc22]).

The article is organized as follows. In Section 2, we define the notations that we use in the rest of the paper and we explain the geometrical assumptions we need to develop our method. In Section 3, we present our method to compute a second order consistent flux using an upwind scheme. Section 4 is dedicated to the numerical scheme. Numerical examples are shown in Section 5.

2 Notations assumptions on the mesh

We present here some notations that will be used in the rest of the paper. Let Ω_j be a cell of the mesh \mathcal{T} paving the domain Ω , we define:

- V_j is the volume of the cell Ω_j ,
- $(\mathbf{x}_r)_{r \in \Omega_j}$ the coordinates of the vertices of the cell j ;
- $\sum_{r \in \Omega_j}$ the sum over all the vertices of the cell j ;
- $r + 1/2$ is the index of the edge between the nodes \mathbf{x}_r and \mathbf{x}_{r+1} , its middle is denoted by $\mathbf{x}_{r+1/2} = (\mathbf{x}_r + \mathbf{x}_{r+1})/2$,

- $\sum_{r+1/2 \in \Omega_j}$ the sum over all edges of the cell j ;
- a *degree of freedom* (denoted as *dof*) is either a node or a mid-edge point;
- $N_j = \sum_{\text{dof} \in \Omega_j} 1$ the number of degrees of freedom in the cell Ω_j ;
- $\sum_{i|\text{dof} \in \Omega_i}$ the sum, for a given degree of freedom, over all the cells that contains this degree of freedom;
- $N_r = \sum_{i|r \in \Omega_i} 1$ the number of cells that contains the given node r ;
- $\sum_{j \in \mathcal{T}}$ the sum over all the cells of the mesh;
- $J = \sum_{j \in \mathcal{T}} 1$ is the number of cells of the mesh;
- h the maximum length of edges of the mesh;
- $I_{k,j}^n$ is the value of the unknown in direction k , in cell j , at iteration n ;
- $I_k = (I_{k,i})_{i \in \mathcal{T}}$ is the vector of the values of the unknown in direction k ;
- $E_j = \sum_{k'=1}^K p_{k'} I_{k',j}$ is the average, in cell j , over the directions;
- $E = (E_i)_{i \in \mathcal{T}}$ is the vector of the averages;
- $\langle \cdot, \cdot \rangle$ the inner product in \mathbb{R}^2 .

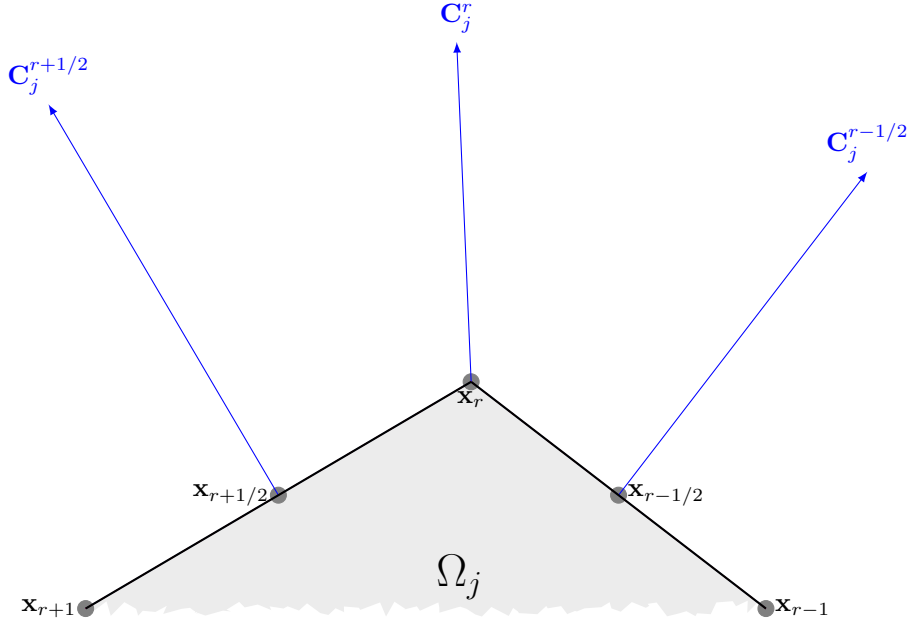


Figure 4: Normal vectors at the nodes and the edges of the cell Ω_j

Let \mathbf{x}_{r-1} , \mathbf{x}_r and \mathbf{x}_{r+1} be 3 consecutive nodes of Ω_j (see Figure 4 for instance). The normal vector to the edge $[\mathbf{x}_r, \mathbf{x}_{r+1}]$ is denoted by $\mathbf{C}_j^{r+1/2} = (\mathbf{x}_{r+1} - \mathbf{x}_r)^\perp$, where for any vector $\boldsymbol{\xi} \in \mathbb{R}^2$:

$$\boldsymbol{\xi} = \begin{pmatrix} \xi_1 \\ \xi_2 \end{pmatrix}, \quad \boldsymbol{\xi}^\perp = \begin{pmatrix} -\xi_2 \\ \xi_1 \end{pmatrix}.$$

Similarly, we define the *normal vector to the node r* as:

$$\mathbf{C}_j^r = \frac{1}{2}(\mathbf{x}_{r+1} - \mathbf{x}_{r-1})^\perp = \frac{1}{2} \left(\mathbf{C}_j^{r+1/2} + \mathbf{C}_j^{r-1/2} \right). \quad (6)$$

Definition (6) was first introduced in [CDDL09]. We also define the matrix:

$$\beta_r = \sum_{i|r \in \Omega_i} \mathbf{C}_i^r \otimes (\mathbf{x}_r - \mathbf{x}_i), \quad (7)$$

We assume that there exists a constant $C_1 \geq 1$ such that, for any *dof* and any cell j :

$$\frac{1}{C_1} h^2 \leq V_j \leq C_1 h^2, \quad N_{\text{dof}} \leq C_1, \quad N_j \leq C_1, \quad (8)$$

Note that by definition we have $\|\mathbf{C}_j^{\text{dof}}\| \leq h$. Moreover, we assume that for any node $r \in \mathcal{T}$ the matrix β_r defined in (7) is positive definite:

$$\forall \boldsymbol{\xi} \in \mathbb{R}^2, \langle \beta_r \boldsymbol{\xi}, \boldsymbol{\xi} \rangle \geq \frac{1}{C_1} h^2 \|\boldsymbol{\xi}\|^2. \quad (9)$$

Thus it is non-singular and we have:

$$\|\beta_r^{-1}\| \leq C_1 \frac{1}{h^2}. \quad (10)$$

Assumption (9) is studied in [Fra12]. We have the following result:

Proposition 2.1. *Let r be an inner node, we have:*

$$\sum_{i|r \in \Omega_i} \mathbf{C}_i^r = 0.$$

We also have the following quadrature formula.

Theorem 2.2. *Let $g \in \mathcal{C}^2(\mathbb{R}^2; \mathbb{R})$. We assume Assumptions (8) are fulfilled. Then, for all $\theta \in [0, 1]$:*

$$\frac{1}{V_j} \int_{\partial\Omega_j} g \mathbf{n} = \frac{1}{V_j} \left[(1 - \theta) \sum_{r \in \Omega_j} g(\mathbf{x}_r) \mathbf{C}_j^r + \theta \sum_{r+1/2 \in \Omega_j} g(\mathbf{x}_{r+1/2}) \mathbf{C}_j^{r+1/2} \right] + O(h). \quad (11)$$

Moreover, the remainder in (11) vanishes if g is an affine function.

Remark 1. *We propose here some explanations on the choice of the parameter θ :*

- $\theta = 0$: node based scheme, consistent but may suffer from cross stencil phenomena (see [BHL21, BDH21]),
- $\theta = 1$: edge-based scheme, useful to implement Dirichlet boundary conditions (see Section 3.2),
- $\theta = 2/3$: better precision. Formula (11) is exact for quadratic functions and the remainder is $O(h^2)$. This choice may allow to have third order convergence (see [BHL24] for instance).

3 Upwind scheme

In this Section, we present a second order consistent approximation of the flux $\int_{\partial\Omega_j} g \langle \mathbf{a}, \mathbf{n} \rangle$, where \mathbf{n} is the outward unit vector to $\partial\Omega_j$, g is a given function and \mathbf{a} is a given velocity field. First we use Theorem 2.2 and we approximate:

$$\int_{\partial\Omega_j} g \langle \mathbf{a}, \mathbf{n} \rangle \approx \theta \sum_{r \in \Omega_j} \langle \mathbf{a}_r, \mathbf{C}_j^r \rangle g_j^r + (1 - \theta) \sum_{r+1/2 \in \Omega_j} \langle \mathbf{a}_{r+1/2}, \mathbf{C}_j^{r+1/2} \rangle g_j^{r+1/2}, \quad (12)$$

where $\mathbf{a}_{\text{dof}} = \mathbf{a}(\mathbf{x}_{\text{dof}})$ and g_j^{dof} is an approximation to $(\mathbf{x}_{\text{dof}})$ in cell j . It is given by an upwind scheme:

$$g_j^{\text{dof}} = \begin{cases} \bar{g}_j^{\text{dof}} & \text{if } \langle \mathbf{a}_{\text{dof}}, \mathbf{C}_j^{\text{dof}} \rangle > 0, \\ \frac{1}{\sum_{i \in \mathcal{A}_{\text{dof}}^+} \langle \mathbf{a}_{\text{dof}}, \mathbf{C}_i^{\text{dof}} \rangle} \sum_{i \in \mathcal{A}_{\text{dof}}^+} \langle \mathbf{a}_{\text{dof}}, \mathbf{C}_i^{\text{dof}} \rangle \bar{g}_i^{\text{dof}} & \text{else,} \end{cases} \quad (13)$$

where: $\mathcal{A}_{\text{dof}}^+ = \{i, \langle \mathbf{a}_{\text{dof}}, \mathbf{C}_i^{\text{dof}} \rangle > 0\}$. The quantity \bar{g}_j^{dof} is a second order approximation of g at point \mathbf{x}_{dof} in cell j that is given by:

$$\bar{g}_j^{\text{dof}} = \begin{cases} g_j - \langle \mathbf{p}_{\text{dof}}, \mathbf{x}_j - \mathbf{x}_{\text{dof}} \rangle & \text{if } |\langle \mathbf{p}_{\text{dof}}, \mathbf{x}_j - \mathbf{x}_{\text{dof}} \rangle| < g_j, \\ g_j & \text{else.} \end{cases} \quad (14)$$

The vector \mathbf{p}_{dof} is an approximation of $-\nabla g$ at point \mathbf{x}_{dof} computed as:

$$\mathbf{p}_r = \beta_r^{-1} \sum_{i|r \in \Omega_i} g_i \mathbf{C}_i^r, \quad \mathbf{p}_{r+1/2} = \frac{\mathbf{p}_r + \mathbf{p}_{r+1}}{2}. \quad (15)$$

Under the assumptions of Section 2, the quantity \mathbf{p}_{dof} defined in (15) is first order consistent with $(-\nabla g)_{\text{dof}}$. Indeed, using a Taylor expansion, we have:

$$g(\mathbf{x}_i) = g(\mathbf{x}_r) + \langle \mathbf{x}_i - \mathbf{x}_r, \nabla g(\mathbf{x}_r) \rangle + O(h^2). \quad (16)$$

Multiplying (16) by \mathbf{C}_i^r , summing the result over the cells around any inner node r and using Lemma 2.1 leads to:

$$\sum_{i|r \in \Omega_i} g(\mathbf{x}_i) \mathbf{C}_i^r = g(\mathbf{x}_r) \underbrace{\sum_{i|r \in \Omega_i} \mathbf{C}_i^r}_{=0} - \beta_r \nabla g(\mathbf{x}_r) + O(h^3), \quad (17)$$

where β_r is defined by (7). Using (10), we have:

$$\beta_r^{-1} \left(\sum_{i|r \in \Omega_i} g(\mathbf{x}_i) \mathbf{C}_i^r \right) = -(\nabla g)(\mathbf{x}_r) + O(h).$$

Moreover, \mathbf{x}_i being the barycenter of the cell i , we have:

$$g(\mathbf{x}_i) = \frac{1}{V_i} \int_{\Omega_i} g + O(h^2). \quad (18)$$

Using (15) (18), we deduce that \mathbf{p}_r is first order consistent with $-(\nabla g)_r$. We easily deduce that $\mathbf{p}_{r+1/2}$ is first order consistent with $-(\nabla g)_{r+1/2}$.

Eventually, we define the second order flux by:

$$\mathcal{F}_j(g, \mathbf{a}) = \frac{\theta}{V_j} \sum_{r \in \Omega_j} \langle \mathbf{a}_r, \mathbf{C}_j^r \rangle g_{j,r} + \frac{1-\theta}{V_j} \sum_{r+1/2 \in \Omega_j} \langle \mathbf{a}_{r+1/2}, \mathbf{C}_j^{r+1/2} \rangle g_{j,r+1/2}, \quad (19)$$

and where $g_{j,\text{dof}}$ is given by (13) (14) (15).

3.1 Properties

We present here the main properties of the flux (12)-(13). The proofs are given in Appendix 7. It is conservative:

Proposition 3.1. *We assume that periodic boundary conditions are imposed on g , then the flux (12)-(13) is conservative:*

$$\sum_{j \in \mathcal{T}} V_j \mathcal{F}_j(g, \mathbf{a}) = 0.$$

Beside, we have the following stability result:

Lemma 3.2. *Under Assumption (8), if $g \geq 0$, and if*

$$\Delta t \leq \frac{1}{2C_1^2} \frac{h}{\|\mathbf{a}\|_{L^\infty(\Omega)}}, \quad (20)$$

then $g_j - \Delta t \mathcal{F}_j(g, \mathbf{a}) \geq 0$.

3.2 Dirichlet boundary conditions

We denote by $\gamma \in \mathcal{C}^0(\partial\Omega)$ the Dirichlet boundary condition:

$$g(t, \mathbf{x}) = \gamma, \quad \text{if } \mathbf{x} \in \partial\Omega, \quad \text{and } \langle \mathbf{a}(\mathbf{x}), \mathbf{n} \rangle < 0. \quad (21)$$

On the boundary of the domain, the vectors $(\mathbf{C}_j^{r+1/2})_{j, r+1/2}$ are aligned with the normal vector to the boundary of the domain \mathbf{n} . This is not the case for the vectors $(\mathbf{C}_j^r)_{j, r}$. Thus we need to set $\theta = 1$ to correctly discretise (21).

Besides, in the cells on the boundary and for the edges on the boundary, we set:

$$g_j^{r+1/2} = \begin{cases} \bar{g}_j^{r+1/2}, & \text{if } \langle \mathbf{a}_{r+1/2}, \mathbf{C}_j^{r+1/2} \rangle > 0, \\ \gamma(\mathbf{x}_{r+1/2}) & \text{else,} \end{cases} \quad (22)$$

where $\bar{g}_j^{r+1/2}$ is given by 14.

Note that the gradients \mathbf{u}_r given by (26) is not well-defined in the corner nodes. Indeed there is only one support cell and thus the matrix β_r (7) has rank 1 and is singular. To overcome this difficulty we compute the gradient \mathbf{u}_r at the corner as the average of the gradients at the other nodes of the support cell.

Remark 2. *In the diffusion regime, the Dirichlet boundary condition is imposed on the whole boundary, thus it is no longer necessary to set $\theta = 1$.*

3.3 Periodic boundary conditions

In the case of periodic boundary conditions, we add some *ghost* cells on the outside of the mesh so as to make it periodic. We then define I on these new cells and we use these values and this new geometric data to compute the $\mathbf{C}_j^{\text{dof}}$ on the boundary of the domain.

4 Numerical scheme

In this Section we present our numerical scheme. The space discretisation is given in Section 4.1. The time discretisation is described in 4.2. The properties and the diffusion limit of the scheme are given in Section 4.3 and Section 4.4.

4.1 Upwind scheme and modified streaming velocity

Equation (5) is integrated over the cell Ω_j . We use the second order upwind flux (19) to approximate the flux:

$$\frac{d}{dt}I_{k,j} + \mathcal{F}_j(I_k, \bar{\omega}_k) + \frac{\sigma_j^t}{\varepsilon^2}I_{k,j} = \frac{\sigma_j^s}{\varepsilon^2} \sum_{k'=1}^K p_{k'} I_{k',j} + q_{k,j}$$

The streaming velocity $\bar{\omega}_{k,\text{dof}}$ is a consistent approximation of ω_k/ε , meaning that:

$$\bar{\omega}_{k,\text{dof}} = \frac{1}{\varepsilon} \omega_k + O(h^2). \quad (23)$$

We want $\bar{\omega}_{k,\text{dof}}$ to be second order consistent with ω_k/ε because we aim at designing a scheme that is second order consistent with (5). Moreover, in order to be consistent with (3) in the diffusion regime, we also impose the following condition:

$$\lim_{\varepsilon \rightarrow 0} \bar{\omega}_{k,\text{dof}} \quad \text{is consistent with} \quad - \left(\frac{\nabla E}{3\sigma^s E} \right)_{\text{dof}}, \quad (24)$$

where E is the average over the directions (see Section 2): $E = \sum_{k'=1}^K I_{k'}/K$. The condition (24) is justified in Section 4.4. Therefore we propose:

$$\bar{\omega}_{k,\text{dof}} = \frac{\varepsilon^2 \omega_k + (\sigma_{\text{dof}}^t)^2 h^3 \mathbf{u}_{\text{dof}}}{\varepsilon^3 + (\sigma_{\text{dof}}^t h)^3}. \quad (25)$$

The quantity \mathbf{u}_{dof} is an approximation of $-\nabla E/(3E)$ at point \mathbf{x}_{dof} . It is given by:

$$\mathbf{u}_r = \frac{1}{3E_r} \beta_r^{-1} \sum_{i|r \in \Omega_i} E_i \mathbf{C}_i^r, \quad E_r = \frac{1}{N_r} \sum_{i|r \in \Omega_i} E_i + h^2, \quad \mathbf{u}_{r+1/2} = \frac{\mathbf{u}_r + \mathbf{u}_{r+1}}{2}, \quad (26)$$

where we recall that β_r is defined in (7). The quantity E_r is an approximation of E at point \mathbf{x}_r . We add a h^2 term in order to make \mathbf{u}_r well defined in the case where all the $(E_i)_i$ vanish.

Lemma 4.1. *Under Assumptions (8) (9) (10), and assuming that the $(I_{k,j})_{k \leq K, j \in \mathcal{T}}$ are nonnegative, we have, for any dof:*

$$\|\mathbf{u}_{\text{dof}}\| \leq \frac{C_1^2}{3h}.$$

Therefore Definition (25) does satisfy (23) and (24). Thus the resulting scheme is nonlinear and second order consistent with (5). Moreover, in the streaming regime, that is to say when $\sigma^t = \sigma^s = 0$, we have exactly $\bar{\omega}_{k,\text{dof}} = \omega_k/\varepsilon$. We also emphasize that $\bar{\omega}_{k,\text{dof}}$ in (25) may be written as a convex combination between the advection velocity ω_k/ε and the "diffusion" velocity \mathbf{u}/σ^s :

$$\bar{\omega}_{k,\text{dof}} = \eta \frac{\omega_k}{\varepsilon} + (1 - \eta) \frac{\mathbf{u}_{\text{dof}}}{\sigma_{\text{dof}}^s}, \quad \eta = \frac{\varepsilon^3}{\varepsilon^3 + (\sigma_{\text{dof}}^t h)^3}.$$

Remark 3 (Discontinuity of the cross sections). *In the case when σ^t is discontinuous, then we choose the mesh such that the discontinuity is located at an interface dof^* . At this interface, σ^t is no longer defined. To overcome this difficulty, we set, at this interface:*

$$\bar{\omega}_{k,\text{dof}^*} = \frac{\omega_k}{\varepsilon}.$$

4.2 Partially implicit time discretisation

We use a partially implicit time discretisation. The streaming term is chosen completely explicit whilst the source and absorption terms are still implicit:

$$\frac{I_{k,j}^{n+1} - I_{k,j}^n}{\Delta t} + \mathcal{F}_j(I_k^n, \bar{\omega}_k^n) + \frac{\sigma_j^t}{\varepsilon^2} I_{k,j}^{n+1} - \frac{\sigma_j^s}{\varepsilon^2} \sum_{k'=1}^K p_{k'} I_{k',j}^{n+1} = q_{k,j} \quad (27)$$

Owing to Sherman-Morrison Lemma 4.2, we can write an explicit formula for $I_{k,j}^{n+1}$. This result is given in Proposition 4.3. Besides, it shows that System (27) can be written as a system without any stiff term. Thus, this system admits a finite and nonzero limit when $\varepsilon \rightarrow 0$. This limit is described in Section 4.4.

Lemma 4.2. *Let $A \in \mathbb{R}^{K \times K}$ be nonsingular, and let $u \in \mathbb{R}^K$, $v \in \mathbb{R}^K$. The matrix $A + u \otimes v$ is nonsingular if and only if $1 + \langle v, A^{-1}u \rangle \neq 0$. Besides, in such a case, its inverse is given by:*

$$(A + u \otimes v)^{-1} = A^{-1} - \frac{1}{1 + \langle v, A^{-1}u \rangle} A^{-1}u \otimes vA^{-1}. \quad (28)$$

Proof. The proof can be found in [Ser02]. □

Proposition 4.3. *Equation (27) is equivalent to:*

$$I_{k,j}^{n+1} = \mu_j^{(1)} (I_k^n - \Delta t \mathcal{F}_j(I_k^n, \bar{\omega}_k^n) + \Delta t q_{k,j}) + \mu_j^{(2)} \sum_{k'=1}^K p_{k'} (I_{k',j}^n - \Delta t \mathcal{F}_j(I_{k'}^n, \bar{\omega}_{k'}^n) + \Delta t q_{k',j}), \quad (29)$$

where:

$$\mu_j^{(1)} = \frac{\varepsilon^2}{\varepsilon^2 + \Delta t \sigma_j^t}, \quad \mu_j^{(2)} = \frac{\Delta t \sigma_j^s}{\varepsilon^2 + \Delta t \sigma_j^t} \times \frac{1}{1 + \Delta t \sigma_j^a}. \quad (30)$$

Proof. Using (30), Equation (27) reads as:

$$I_{k,j}^{n+1} - \frac{\Delta t \sigma_j^s}{\varepsilon^2 + \Delta t \sigma_j^t} \sum_{k'=1}^K p_{k'} I_{k',j}^{n+1} = \mu_j^{(1)} (I_k^n - \Delta t \mathcal{F}_j(I_k^n, \bar{\omega}_k^n) + \Delta t q_{k,j}). \quad (31)$$

Equation (31) can be set under the following form:

$$(i_K - \lambda_j v \otimes p) I_j^{n+1} = b_j, \quad I_j^{n+1} = \begin{pmatrix} I_{1,j}^{n+1} \\ \vdots \\ I_{K,j}^{n+1} \end{pmatrix} \in \mathbb{R}^K, \quad p = \begin{pmatrix} p_1 \\ \vdots \\ p_K \end{pmatrix} \in \mathbb{R}^K, \quad v = \begin{pmatrix} 1 \\ \vdots \\ 1 \end{pmatrix} \in \mathbb{R}^K, \quad (32)$$

where i_K is the identity matrix of size K and:

$$\lambda_j = \frac{\Delta t \sigma_j^s}{\varepsilon^2 + \Delta t \sigma_j^t}, \quad b_{k,j} = \mu_j^{(1)} (I_k^n - \Delta t \mathcal{F}_j(I_k^n, \bar{\omega}_k^n) + \Delta t q_{k,j}).$$

Moreover, owing to (4), we have:

$$1 - \lambda_j \langle v, p \rangle = 1 - \frac{\Delta t \sigma_j^s}{\varepsilon^2 + \Delta t \sigma_j^t} > 0.$$

Therefore, according to Lemma 4.2, the matrix of System (32) is nonsingular and its inverse is given by:

$$(i_K - \lambda_j v \otimes p)^{-1} = i_K + \frac{\lambda_j}{1 - \frac{\Delta t \sigma_j^s}{\varepsilon^2 + \Delta t \sigma_j^t}} v \otimes p = i_K + \frac{\Delta t \sigma_j^s}{\varepsilon^2 + \Delta t \varepsilon^2 \sigma_j^a} v \otimes p.$$

Thus Equation (31) becomes:

$$I_{k,j}^{n+1} = \mu_j^{(1)} (I_k^n - \Delta t \mathcal{F}_j(I_k^n, \bar{\omega}_k^n) + \Delta t q_{k,j}) + \underbrace{\mu_j^{(1)} \frac{\Delta t \sigma_j^s}{\varepsilon^2 + \Delta t \varepsilon^2 \sigma_j^a}}_{=\mu_j^{(2)}} \sum_{k'=1}^K p_{k'} (I_{k',j}^n - \Delta t \mathcal{F}_j(I_{k'}^n, \bar{\omega}_{k'}^n) + \Delta t q_{k',j}).$$

The result is proved. \square

Therefore $I_{k,j}^{n+1}$ writes explicitly as a function of the quantities at iteration n . Besides, if $q = \sigma^a = 0$ then $\mu_j^{(1)} + \mu_j^{(2)} = 1$ and $I_{k,j}^{n+1}$ simply reads as a convex combination between the anisotropic and isotropic dynamics. We observe in Section 5 that the scheme (29) is indeed second order convergent. Moreover, the positivity of the solution is preserved under a classical CFL condition (see Proposition 4.6 below).

Remark 4. *The scheme (29) has the same computational cost as an explicit scheme. There is no stiff term. No fixed point iteration is required, no linear system needs to be solved. Thus each time iteration is very fast to compute and there is no need for an acceleration procedure in the diffusion limit.*

4.3 Properties

In this section, we present the properties of the scheme (27). We first detail the conservation property (Proposition 4.4), then we give an intermediary result (Lemma 4.5) that is used in the proof of the CFL condition (Proposition 4.6).

Proposition 4.4. *We assume periodic boundary conditions are imposed. If $\sigma^a = 0$, then the scheme (27) is conservative:*

$$\sum_{j \in \mathcal{T}} V_j E_j^{n+1} = \sum_{j \in \mathcal{T}} V_j E_j^n + \Delta t \sum_{j \in \mathcal{T}} V_j \sum_{k'=1}^K p_{k'} q_{k',j}.$$

Proof. This result is a direct consequence of Lemma 3.1. We multiply Equation (27) by p_k and we sum over the directions, this gives:

$$\frac{1}{\Delta t} \left[\sum_{k'=1}^K p_{k'} I_{k',j}^{n+1} - \sum_{k'=1}^K p_{k'} I_{k',j}^n - \Delta t \sum_{k'=1}^K p_{k'} q_{k',j} \right] + \sum_{k'=1}^K p_{k'} \mathcal{F}_j(I_{k'}^n, \bar{\omega}_{k'}^n) = 0. \quad (33)$$

We multiply (33) by V_j and we sum over the cells, which leads to:

$$\frac{1}{\Delta t} \sum_{j \in \mathcal{T}} V_j \left[\sum_{k'=1}^K p_{k'} I_{k',j}^{n+1} - \sum_{k'=1}^K p_{k'} I_{k',j}^n - \Delta t \sum_{k'=1}^K p_{k'} q_{k',j} \right] + \sum_{k'=1}^K p_{k'} \sum_{j \in \mathcal{T}} V_j \mathcal{F}_j(I_{k'}^n, \bar{\omega}_{k'}^n) = 0.$$

Lemma 3.1 states that:

$$\sum_{j \in \mathcal{T}} V_j \mathcal{F}_j(I_{k'}^n, \bar{\omega}_{k'}^n) = 0.$$

The result is proved. \square

Lemma 4.5. *Under the assumptions of Lemma 4.1, we have, for any dof and any direction k :*

$$\|\bar{\omega}_{k,dof}\| \leq 4 \max \left(1, \frac{C_1^2}{3} \right) \frac{1}{\sigma_{dof}^t h + \varepsilon}.$$

Proof. We use Lemma 4.1 and $\|\boldsymbol{\omega}_k\| \leq 1$ in (25). This gives:

$$\|\bar{\boldsymbol{\omega}}_{k,\text{dof}}\| \leq \max\left(1, \frac{C_1^2}{3}\right) \frac{\varepsilon^2 + (\sigma_{\text{dof}}^t h)^2}{\varepsilon^3 + (\sigma_{\text{dof}}^t h)^3} \leq 4 \max\left(1, \frac{C_1^2}{3}\right) \frac{1}{\sigma_{\text{dof}}^t h + \varepsilon}. \quad (34)$$

The result is proved. \square

Proposition 4.6. *Under Assumptions (8) (9) (10), if $(I_{k,j}^n)_{k,j}$ and q are nonnegative, and if:*

$$\Delta t \leq C_{4.6} \left(\varepsilon h + h^2 \min_{\text{dof} \in \mathcal{T}} \sigma_{\text{dof}}^t \right), \quad (35)$$

with $C_{4.6} = \left[8C_1^2 \max\left(1, \frac{C_1^2}{3}\right) \right]^{-1}$, then $I_{k,j}^{n+1}$ is nonnegative for all k, j .

Proof. Recalling that q , $\mu^{(1)}$ and $\mu^{(2)}$ are nonnegative and using Lemma 3.2 and Lemma 4.5 gives the desired result. \square

4.4 AP property and limit scheme

In this Section, we explain why the scheme (29) is AP. More precisely, we study the limit of the scheme (29) as ε goes to 0. First, one can easily see that:

$$\mu_j^{(1)} \xrightarrow{\varepsilon \rightarrow 0} 0. \quad (36)$$

Besides, using $\sigma^t = \sigma^s + \varepsilon^2 \sigma^a$ leads to:

$$\mu_j^{(2)} \xrightarrow{\varepsilon \rightarrow 0} \frac{1}{1 + \Delta t \sigma^a}. \quad (37)$$

Therefore, combining (29) and (36) (37) gives the following limit as ε vanishes:

$$I_{k,j}^{n+1} = \frac{1}{1 + \Delta t \sigma^a} \sum_{k'=1}^K p_{k'} (I_{k',j}^n - \Delta t \mathcal{F}_j(I_{k'}^n, \bar{\boldsymbol{\omega}}_{k'}^n) + \Delta t q_{k',j}).$$

Thus I is isotropic:

$$I_{k,j}^{n+1} = \sum_{k'=1}^K p_{k'} I_{k',j}^{n+1} = E_j^{n+1}.$$

In addition, when ε vanishes, the velocity field does not depend on ω_k anymore and so is the flux:

$$\bar{\boldsymbol{\omega}}_{k,\text{dof}} = \frac{\mathbf{u}_{\text{dof}}}{\sigma_{\text{dof}}^s}, \quad \mathcal{F}_j(I_k^n, \bar{\boldsymbol{\omega}}_k^n) = \mathcal{F}_j\left(E^n, \frac{\mathbf{u}^n}{\sigma^s}\right).$$

Therefore, as ε goes to 0, Equation (29) becomes:

$$(1 + \Delta t \sigma^a) E_j^{n+1} = E_j^n - \Delta t \mathcal{F}_j\left(E^n, \frac{\mathbf{u}^n}{\sigma^s}\right) + \Delta t \sum_{k'=1}^K p_{k'} q_{k',j},$$

which may be written as:

$$\frac{E_j^{n+1} - E_j^n}{\Delta t} + \mathcal{F}_j\left(E^n, \frac{\mathbf{u}^n}{\sigma^s}\right) + \sigma_j^a E_j^{n+1} = \sum_{k'=1}^K p_{k'} q_{k',j}. \quad (38)$$

As \mathbf{u} is consistent with $-\nabla E/(3E)$, the flux is consistent with $-\text{div}[E \times \nabla E/(3\sigma^s E)] = -\text{div}[\nabla E/(3\sigma^s)]$. Therefore (38) is consistent with (3). It is the second order scheme from [BHL24].

5 Numerical results

In this Section we present some numerical examples to illustrate the good properties of our method. We use a quadrature of *Equal Weights* from [Car]. The weights $(p_k)_{1 \leq k \leq K}$ are equal to $1/K$ and the number of directions has to be of the following form $K = 4N^2$ with $N \in \mathbb{N}$.

In the first three test cases, we compute analytical solutions of (2) and we perform a convergence analysis (Sections 5.1, 5.2, 5.3) on cartesian meshes (uniform grids) and random meshes (see Figure 5). Denoting by \tilde{I} the exact solution and t_f the final time, the error is computed the following way:

$$\text{error} = \max_{1 \leq k \leq K} \left(\frac{\sum_{j \in \mathcal{T}} V_j |I_{k,j} - \tilde{I}(t_f, \mathbf{x}_j, \boldsymbol{\omega}_k)|}{\sum_{j \in \mathcal{T}} V_j \tilde{I}(t_f, \mathbf{x}_j, \boldsymbol{\omega}_k)} \right).$$

We also compute the solution of a *Lattice problem* defined in [BH05] in Section 5.4. Eventually we present our results for a test case from [KFJ16].

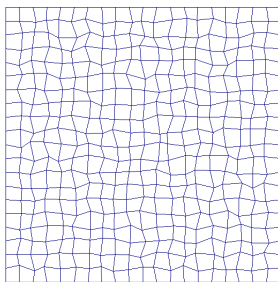


Figure 5: Random mesh.

5.1 Free streaming regime

In this test case, we choose $\sigma^s = \sigma^a = 0$, $q = 0$ and $\varepsilon = 1$. The exact solution is given by:

$$I(t, \mathbf{x}, \boldsymbol{\omega}) = \exp\left(-100 \|\mathbf{x} - t\boldsymbol{\omega} - \mathbf{x}_0\|^2\right), \quad \mathbf{x}_0 = (1, 1).$$

Dirichlet boundary conditions are imposed (see Section 3.2). We choose $K = 4$ directions. The computational domain is $\Omega = [0, 2]^2$. We set $\theta = 1$. Figure 6 shows the error curve at final time $t_f = 0.03$ and $\Delta t = h^2$. Indeed, as the scheme (29) is first order consistent in time, we need to set $\Delta t = O(h^2)$ in order to make the consistency error decrease as h^2 . We see that our method gives the expected rate of convergence.

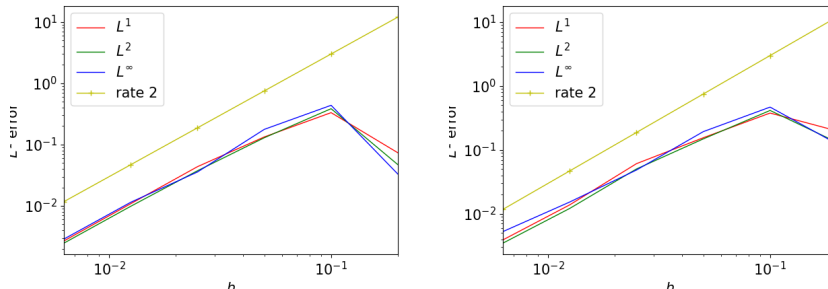


Figure 6: Error on cartesian (left) and random (right) meshes.

5.2 Diffusion regime

In this test case, we choose $\sigma^s = 1$, $\sigma^a = q = 0$ and $\varepsilon = 0$. The exact solution is the fundamental solution of the diffusion equation:

$$\partial_t E - \frac{1}{3} \Delta E = 0, \quad E(t, \mathbf{x}) = \frac{3}{4\pi(t+t_0)} \exp\left(-3 \frac{\|\mathbf{x} - \mathbf{x}_0\|^2}{4(t+t_0)}\right),$$

with $t_0 = 0.01$ and $\mathbf{x}_0 = (1, 1)$. The computational domain is $\Omega = [0, 2]^2$. Dirichlet boundary conditions are imposed. We choose $K = 4$ directions and $\theta = 1/2$. The timestep is given by $\Delta t = h^2$ and the final time is $t_f = 0.03$. Figure 7 shows the error curves. The right convergence rate is recovered.

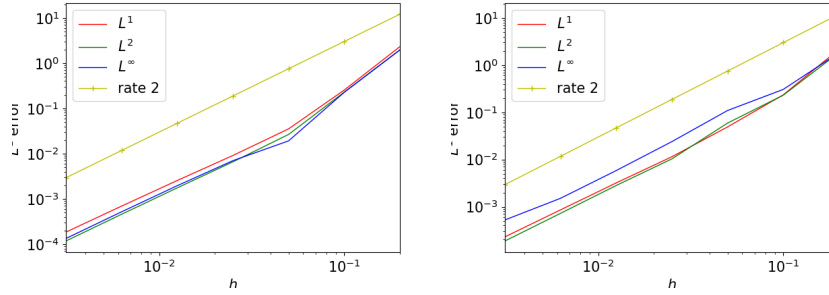


Figure 7: Error on cartesian (left) and random (right) meshes.

5.3 Manufactured test case

We choose $\varepsilon = 1$. The analytical solution of this test case is given by:

$$I(t, x, y, \boldsymbol{\omega}) = e^t (10 + \sin(2\pi x) + \sin(2\pi y) + \langle \boldsymbol{\omega}, \mathbf{f} \rangle), \quad \mathbf{f} = (1, -1),$$

and the absorption coefficients are given by:

$$\sigma^t(x, y) = 2 + (\sin(2\pi x) + \sin(2\pi y))^2, \quad \sigma^s = 0.1.$$

We compute the source term $q(t, x, y, \boldsymbol{\omega})$ so as to satisfy Equation (2). Periodic boundary conditions are imposed. We set $K = 4$. Figure 8 displays the error curves with the second order scheme at time $t_f = 0.01$ and $\Delta t = h^2$ and $\theta = 1/2$.

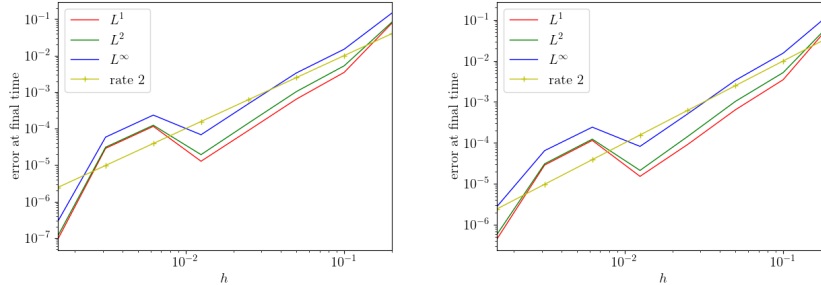


Figure 8: Error on cartesian meshes (left) and random meshes (right).

5.4 Lattice problem

This test case is borrowed from [BH05]. The computational domain is $\Omega = [0, 7]^2$. The initial condition is 0 and $\varepsilon = 1$. The source term is $q = 1_{[3,4] \times [3,4]}$. Homogeneous Dirichlet boundary conditions are imposed. We set $\theta = 1$. The final time is $t_f = 3.2$ and the time step is $\Delta t = 0.01$. The absorption coefficients are:

$$\sigma^t = 10 \times 1_{\Omega_A}, \quad \sigma^s = 1 - 1_{\Omega_A}.$$

The domain Ω_A is pictured in red color in Figure 9.

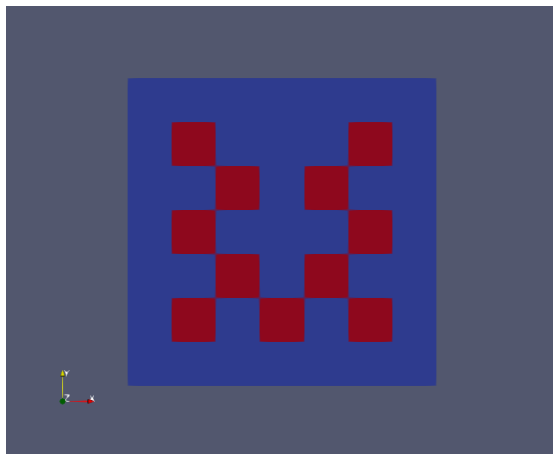


Figure 9: The domain Ω_A in red color.

Some numerical solutions are plotted in the following Figures. The log scale map is limited to seven orders of magnitude: we display with the same blue color all the regions where the solution is smaller or equal to 10^{-7} .

Figures 10, 11 and 12 display the numerical solution with $K = 4$, $K = 144$ and $K = 484$ respectively. We see that we recover the results of [BH05].

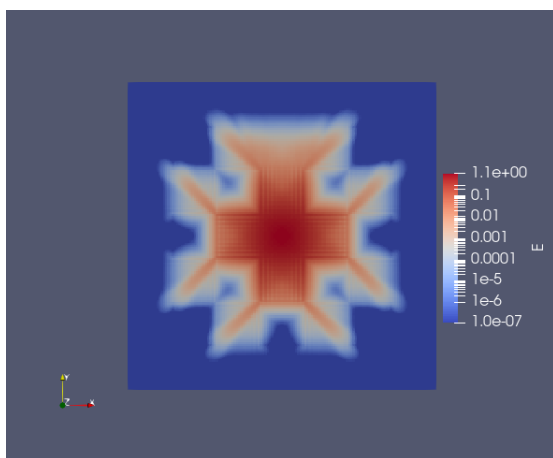


Figure 10: Numerical solution (in log scale) at time $t_f = 3.2$ on a cartesian mesh of size 140×140 and with $K = 4$.

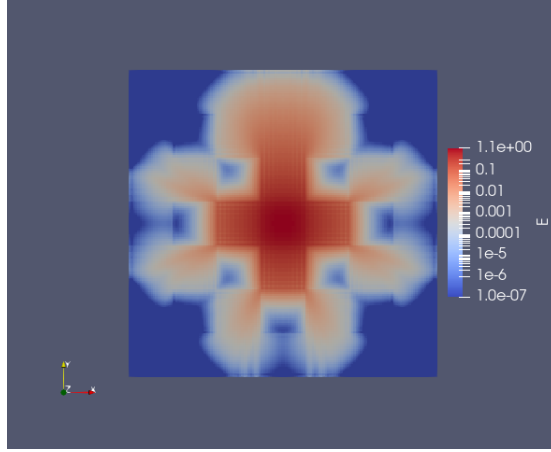


Figure 11: Numerical solution (in log scale) at time $t_f = 3.2$ on a cartesian mesh of size 140×140 and with $K = 144$.

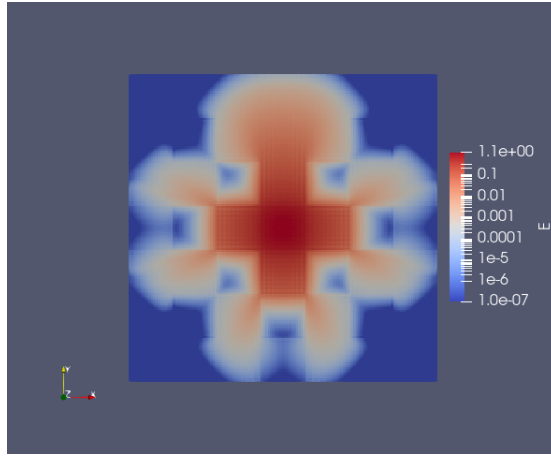


Figure 12: Numerical solution (in log scale) at time $t_f = 3.2$ on a cartesian mesh of size 140×140 and with $K = 484$.

5.5 Variable scattering test case

Here we compute the solution of the *variable scattering* test case from [KFJ16]. The domain is $[-1, 1]^2$, the final time is $t_f = 0.005$ and we set $\varepsilon = 0.01$ and $\sigma^a = q = 0$. The initial condition and the cross section are given by:

$$I(t = 0, x, y, \omega_x, \omega_y) = \frac{1}{0.04\pi} \exp\left(-\frac{x^2 + y^2}{0.04}\right), \quad \sigma^s(x, y) = \begin{cases} c^4(c^2 - 2)^2 & \text{if } c = \sqrt{x^2 + y^2} < 1, \\ 1 & \text{else.} \end{cases}$$

The solution is almost 0 near the boundary, so we impose periodic boundary conditions. We set $\theta = 1/2$. Figure 13 shows the solution E on a uniform grid of size $N_x = N_y = 200$ with $\Delta t = 10^{-3}$. We do recover the solution from [KFJ16].

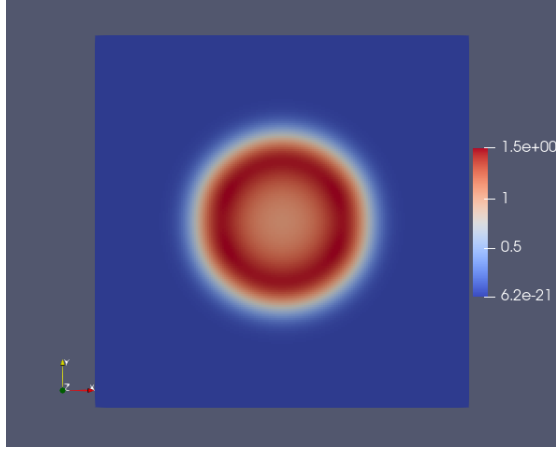


Figure 13: Numerical solution E at time $t_f = 0.005$ on a cartesian mesh of size 200×200 and with $K = 64$.

6 Conclusion and future work

In this paper we have presented a scheme that is asymptotic preserving, positive under a classical CFL condition that depend on the regime, conservative and second order consistent in space. Besides its computational cost is quite low as there is no linear system to solve nor fixed point iteration to compute.

Several extensions to this work are possible. First, the method can be easily adapted to $3D$ unstructured meshes. Indeed, the $3D$ formulas for the node vectors $(\mathbf{C}_j^r)_{j,r}$ are given in [CDDL09]. The $3D$ equivalent of the vectors $(\mathbf{C}_j^{r+1/2})_{j,r+1/2}$ are nothing but normal vectors to the faces. In addition, we have seen in Proposition 4.3 that the intensity at iteration $n + 1$ can be explicitly computed as a function of the quantities at iteration n . This property will allow us to design a scheme to solve efficiently the transport equation coupled with matter. This is an ongoing work.

7 Appendix

7.1 Proof of Lemma 3.1

First, we have:

$$\sum_{j \in \mathcal{T}} V_j \mathcal{F}_j(g, \mathbf{a}) = (1 - \theta) \sum_{j \in \mathcal{T}} \sum_{r \in \Omega_j} \langle \mathbf{C}_j^r, \mathbf{a}_r \rangle g_j^r + \theta \sum_{j \in \mathcal{T}} \sum_{r+1/2 \in \Omega_j} \langle \mathbf{C}_j^{r+1/2}, \mathbf{a}_{r+1/2} \rangle g_j^{r+1/2}. \quad (39)$$

Now we prove:

$$\sum_{j \in \mathcal{T}} \sum_{r \in \Omega_j} \langle \mathbf{C}_j^r, \mathbf{a}_r \rangle g_j^r = 0. \quad (40)$$

Indeed, exchanging the sums over the cells and over the nodes leads to:

$$\sum_{j \in \mathcal{T}} \sum_{r \in \Omega_j} \langle \mathbf{C}_j^r, \mathbf{a}_r \rangle g_j^r = \sum_{r \in \mathcal{T}} \sum_{i | r \in \Omega_i} \langle \mathbf{C}_i^r, \mathbf{a}_r \rangle g_i^r. \quad (41)$$

Besides, using (13), the last sum in (41) can be written as:

$$\sum_{i|r \in \Omega_i} g_i^r \langle \mathbf{C}_i^r, \mathbf{a}_r \rangle = \sum_{i \in I_r^+} \bar{g}_i^r \langle \mathbf{C}_i^r, \mathbf{a}_r \rangle + \sum_{i \in I_r^-} \left(\underbrace{\frac{1}{\sum_{\ell \in I_r^+} \langle \mathbf{a}_r, \mathbf{C}_\ell^r \rangle} \sum_{\ell \in I_r^+} \langle \mathbf{a}_r, \mathbf{C}_\ell^r \rangle \bar{g}_\ell^r}_{\text{independent from } i} \right) \langle \mathbf{C}_i^r, \mathbf{a}_r \rangle. \quad (42)$$

The quantity:

$$\frac{1}{\sum_{\ell \in I_r^+} \langle \mathbf{a}_r, \mathbf{C}_\ell^r \rangle} \sum_{\ell \in I_r^+} \langle \mathbf{a}_r, \mathbf{C}_\ell^r \rangle \bar{g}_\ell^r$$

being independent from i , we can remove it from the sum $\sum_{i \in I_r^-}$ in (42) and (42) reads as:

$$\sum_{i|r \in \Omega_i} g_i^r \langle \mathbf{C}_i^r, \mathbf{a}_r \rangle = \sum_{i \in I_r^+} \bar{g}_i^r \langle \mathbf{C}_i^r, \mathbf{a}_r \rangle + \left(\sum_{i \in I_r^+} \langle \mathbf{a}_r, \mathbf{C}_i^r \rangle \bar{g}_i^r \right) \frac{1}{\sum_{i \in I_r^+} \langle \mathbf{a}_r, \mathbf{C}_i^r \rangle} \sum_{i \in I_r^-} \langle \mathbf{a}_r, \mathbf{C}_i^r \rangle. \quad (43)$$

Besides, owing to Lemma 2.1, we have:

$$\sum_{i \in I_r^-} \mathbf{C}_i^r = - \sum_{i \in I_r^+} \mathbf{C}_i^r. \quad (44)$$

Computing the inner product of (44) with \mathbf{a}_r gives:

$$\sum_{i \in I_r^-} \langle \mathbf{a}_r, \mathbf{C}_i^r \rangle = - \sum_{i \in I_r^+} \langle \mathbf{a}_r, \mathbf{C}_i^r \rangle, \quad \text{and thus: } \frac{1}{\sum_{i \in I_r^+} \langle \mathbf{a}_r, \mathbf{C}_i^r \rangle} \sum_{i \in I_r^-} \langle \mathbf{a}_r, \mathbf{C}_i^r \rangle = -1. \quad (45)$$

Inserting (45) in (43) leads to:

$$\sum_{i|r \in \Omega_i} g_i^r \langle \mathbf{C}_i^r, \mathbf{a}_r \rangle = 0. \quad (46)$$

Collecting (41) and (46) proves (40).

Using similar arguments, we can easily show:

$$\sum_{j \in \mathcal{T}} \sum_{r+1/2 \in \Omega_j} \langle \mathbf{C}_j^{r+1/2}, \mathbf{a}_{r+1/2} \rangle g_j^{r+1/2} = 0. \quad (47)$$

Inserting (40) and (47) in (39) gives the desired result.

7.2 Proof of Lemma 3.2

First, we define:

$$R_j^+ = \{r, \langle \mathbf{C}_j^r, \mathbf{a}_r \rangle > 0\}, \quad R_j^- = \{r, \langle \mathbf{C}_j^r, \mathbf{a}_r \rangle \leq 0\},$$

and:

$$\tilde{R}_j^+ = \{r+1/2, \langle \mathbf{C}_j^{r+1/2}, \mathbf{a}_{r+1/2} \rangle > 0\}, \quad \tilde{R}_j^- = \{r+1/2, \langle \mathbf{C}_j^{r+1/2}, \mathbf{a}_{r+1/2} \rangle \leq 0\}.$$

Using these definitions, we easily have:

$$g_j - \Delta t \mathcal{F}_j(g, \mathbf{a}) \geq g_j - \frac{\Delta t}{V_j} \left[(1-\theta) \sum_{r \in R_j^+} \langle \mathbf{a}_r, \mathbf{C}_j^r \rangle \bar{g}_j^r + \theta \sum_{r+1/2 \in \tilde{R}_j^+} \langle \mathbf{a}_{r+1/2}, \mathbf{C}_j^{r+1/2} \rangle \bar{g}_j^{r+1/2} \right].$$

According to (14), we have $\bar{g}_j^{\text{dof}} \leq 2g_j$. This leads to:

$$g_j - \Delta t \mathcal{F}_j(g, \mathbf{a}) \geq g_j \left(1 - \frac{2\Delta t}{V_j} \left[(1 - \theta) \sum_{r \in R_j^+} \langle \mathbf{a}_r, \mathbf{C}_j^r \rangle + \theta \sum_{r+1/2 \in \bar{R}_j^+} \langle \mathbf{a}_{r+1/2}, \mathbf{C}_j^{r+1/2} \rangle \right] \right). \quad (48)$$

Besides, using Assumption (8), we have:

$$\frac{\Delta t}{V_j} \left[(1 - \theta) \sum_{r \in R_j^+} \langle \mathbf{a}_r, \mathbf{C}_j^r \rangle + \theta \sum_{r+1/2 \in \bar{R}_j^+} \langle \mathbf{a}_{r+1/2}, \mathbf{C}_j^{r+1/2} \rangle \right] \leq C_1^2 \Delta t \frac{\|\mathbf{a}\|_{L^\infty(\Omega)}}{h}. \quad (49)$$

Collecting (48) and (49) gives the result.

7.3 Proof of Lemma 4.1

As the $(I_{k,j})_{k \leq K, j \in \mathcal{T}}$ are nonnegative, the $(E_j)_{j \in \mathcal{T}}$ are also nonnegative and we have:

$$\frac{\sum_{i|r \in \Omega_i} E_i}{E_r} \leq N_r \leq C_1.$$

Therefore, using Assumption (8) we have:

$$\left\| \frac{1}{E_r} \sum_{i|r \in \Omega_i} E_i \mathbf{C}_i^r \right\| \leq C_1 h.$$

Using (10) gives the result.

References

- [ACE⁺22] Pierre Anguill, Patricia Cargo, Cedric Enaux, Philippe Hoch, Emmanuel Labourasse, and Gerald Samba. An asymptotic preserving method for the linear transport equation on general meshes. *Journal of Computational Physics*, 450:110859, 2022.
- [Ada01] M.L. Adams. Discontinuous finite element transport solutions in thick diffusive problems. *Nuclear Science and Engineering*, 137(3):298 – 333, 2001.
- [BCHS20] Aude Bernard-Champmartin, Philippe Hoch, and Nicolas Seguin. Stabilité locale et montée en ordre pour la reconstruction de quantités volumes finis sur maillages coniques non-structurés en dimension 2. Research report, CEA, CEA/DAM/DIF, Bruyères-le-Châtel, France ; Univ-Rennes1 ; Université Paris 6, March 2020. <https://hal.archives-ouvertes.fr/hal-02497832>.
- [BCWA] T S Bailey, J H Chang, J S Warsa, and M L Adams. A piecewise bi-linear discontinuous finite element spatial discretization of the sn transport equation.
- [BDH21] Xavier Blanc, Vincent Delmas, and Philippe Hoch. Asymptotic preserving schemes on conical unstructured 2d meshes. *International Journal for Numerical Methods in Fluids*, 93(8):2763–2802, 2021.
- [BFR16] Sebastiano Boscarino, Francis Filbet, and Giovanni Russo. High order semi-implicit schemes for time dependent partial differential equations. *Journal of Scientific Computing*, 68, 09 2016.
- [BGPS88] C Bardos, F Golse, B Perthame, and R Sentis. The nonaccretive radiative transfer equations: Existence of solutions and rosseland approximation. *Journal of Functional Analysis*, 77(2):434–460, 1988.

- [BH05] Thomas A. Brunner and James Paul Holloway. Two-dimensional time dependent Riemann solvers for neutron transport. *J. Comput. Phys.*, 210(1):386–399, 2005.
- [BHL21] Xavier Blanc, Philippe Hoch, and Clément Lasuen. An asymptotic preserving scheme for the M1 model on conical meshes. working paper or preprint, 2021.
- [BHL24] Xavier Blanc, Philippe Hoch, and Clément Lasuen. Composite finite volume schemes for the diffusion equation on unstructured meshes. *Computers and Mathematics with Applications*, 156:207–217, 2024.
- [BR09] Sebastiano Boscarino and Giovanni Russo. On a class of uniformly accurate imex runge–kutta schemes and applications to hyperbolic systems with relaxation. *SIAM Journal on Scientific Computing*, 31(3):1926–1945, 2009.
- [Car] B G Carlson. Transport theory: Discrete ordinates quadrature over the unit sphere.
- [Cas04] John Castor. *Radiation Hydrodynamics*. Cambridge University Press, 2004.
- [CDDL09] G. Carré, S. Del Pino, B. Després, and E. Labourasse. A cell-centered Lagrangian hydrodynamics scheme on general unstructured meshes in arbitrary dimension. *J. Comput. Phys.*, 228(14):5160–5183, 2009.
- [CS16] F. Chaland and G. Samba. Discrete ordinates method for the transport equation preserving one-dimensional spherical symmetry in two-dimensional cylindrical geometry. *Nuclear Science and Engineering*, 182(4):417–434, 2016.
- [CZ67] K.M. Case and P.F. Zweifel. *Linear Transport Theory*. Addison-Wesley series in nuclear engineering. Addison-Wesley Publishing Company, 1967.
- [EG23] Alexandre Ern and Jean-Luc Guermond. Invariant-domain preserving high-order time stepping: Ii. imex schemes. *SIAM Journal on Scientific Computing*, 45(5):A2511–A2538, 2023.
- [EHW21] Lukas Einkemmer, Jingwei Hu, and Yubo Wang. An asymptotic-preserving dynamical low-rank method for the multi-scale multi-dimensional linear transport equation. *Journal of Computational Physics*, 439:110353, 2021.
- [Fra12] Emmanuel Franck. *Construction et analyse numérique de schema asymptotic preserving sur maillages non structurés. Application au transport linéaire et aux systèmes de Friedrichs*. PhD thesis, Université Pierre et Marie Curie - Paris VI, 2012.
- [GPR20] Jean-Luc Guermond, Bojan Popov, and Jean Ragusa. Positive and asymptotic preserving approximation of the radiation transport equation. *SIAM Journal on Numerical Analysis*, 58(1):519–540, 2020.
- [Hoc22] Philippe Hoch. Nodal extension of Approximate Riemann Solvers and nonlinear high order reconstruction for finite volume method on unstructured polygonal and conical meshes: the homogeneous case. working paper or preprint, February 2022.
- [JL96] Shi Jin and C.David Levermore. Numerical schemes for hyperbolic conservation laws with stiff relaxation terms. *Journal of Computational Physics*, 126(2):449 – 467, 1996.
- [JPT00] Shi Jin, Lorenzo Pareschi, and Giuseppe Toscani. Uniformly accurate diffusive relaxation schemes for multiscale transport equations. *SIAM Journal on Numerical Analysis*, 38(3):913–936, 2000.
- [JS10] Shi Jin and Yingzhe Shi. A micro-macro decomposition-based asymptotic-preserving scheme for the multispecies boltzmann equation. *SIAM Journal on Scientific Computing*, 31(6):4580–4606, 2010.

- [KFJ16] Kerstin Kupper, Martin Frank, and Shi Jin. An asymptotic preserving two-dimensional staggered grid method for multiscale transport equation. *SIAM Journal on Numerical Analysis*, 54(1):440–461, 2016.
- [Kla98] Axel Klar. An asymptotic-induced scheme for nonstationary transport equations in the diffusive limit. *SIAM Journal on Numerical Analysis*, 35(3):1073–1094, 1998.
- [LFH19] M. Paul Laiu, Martin Frank, and Cory D. Hauck. A positive asymptotic-preserving scheme for linear kinetic transport equations. *SIAM Journal on Scientific Computing*, 41(3):A1500–A1526, 2019.
- [IM89] Edward W larsen and J.E. Morel. Asymptotic solutions of numerical transport problems in optically thick, diffusive regimes ii. *Journal of Computational Physics*, 83(1):212–236, 1989.
- [LM08] Mohammed Lemou and Luc Mieussens. A new asymptotic preserving scheme based on micro-macro formulation for linear kinetic equations in the diffusion limit. *SIAM J. Scientific Computing*, 31:334–368, 01 2008.
- [LM10] Jian-Guo Liu and Luc Mieussens. Analysis of an asymptotic preserving scheme for linear kinetic equations in the diffusion limit. *SIAM Journal on Numerical Analysis*, 48(4):1474–1491, 2010.
- [MM84] Dimitri Mihalas and Barbara Weibel Mihalas. *Foundations of radiation hydrodynamics*. Oxford University Press, New York, 1984.
- [RJLM⁺88] Dautray Robert, Lions Jacques-Louis, Artola Michel, Cessenat Michel, Scheurer Bruno, and Robert Dautray. *Analyse mathématique et calcul numérique pour les sciences et les techniques . Volume 8, Évolution, semi-groupe, variationnel / Robert Dautray, Jacques-Louis Lions Michel Artola, Michel Cessenat, Bruno Scheurer*. Collection Enseignement - INSTN CEA. Masson, Paris Milan Barcelone [etc, [nouvelle édition] edition, 1988.
- [Ser02] Denis Serre. *Matrices: Theory and applications*. 2002.